Monthly Notices
of the
ROYAL ASTRONOMICAL SOCIETY

Mon. Not. R. Astron. Soc. **414,** 677–690 (2011) doi:10.1111/j.1365-2966.2011.18433.x

Radiatively efficient accreting black holes in the hard state: the case study of H1743−322

M. Coriat,[1⋆†] S. Corbel,[1,2] L. Prat,[1] J. C. A. Miller-Jones,[3,4] D. Cseh,[1]
A. K. Tzioumis,[5] C. Brocksopp,[6] J. Rodriguez,[1] R. P. Fender[7] and G. R. Sivakoff[8]

[1]*Laboratoire AIM, CEA-IRFU/CNRS/Université Paris Diderot, CEA Saclay, F-91191 Gif-sur-Yvette, France*
[2]*Institut Universitaire de France, 75005 Paris, France*
[3]*NRAO Headquarters, 520 Edgemont Road, Charlottesville, VA 22903, USA*
[4]*International Centre for Radio Astronomy Research – Curtin University, GPO Box U1987, Perth, WA 6845, Australia*
[5]*Australia Telescope National Facility, CSIRO, PO Box 76, Epping, NSW 1710, Australia*
[6]*Mullard Space Science Laboratory, University College London, Holmbury St. Mary, Dorking, Surrey RH5 6NT*
[7]*School of Physics and Astronomy, University of Southampton, Highfield, Southampton SO17 1BJ*
[8]*Department of Astronomy, University of Virgina, PO Box 400325, Charlottesville, VA 22904-4325, USA*

Accepted 2011 January 26. Received 2011 January 26; in original form 2010 June 9

ABSTRACT

In recent years, much effort has been devoted to unravelling the connection between the accretion flow and the jets in accreting compact objects. In the present work, we report new constraints on these issues, through the long-term study of the radio and X-ray behaviour of the black hole candidate H1743−322. This source is known to be one of the 'outliers' of the universal radio/X-ray correlation, i.e. a group of accreting stellar-mass black holes displaying fainter radio emission for a given X-ray luminosity than expected from the correlation. Our study shows that the radio and X-ray emission of H1743−322 are strongly correlated at high luminosity in the hard spectral state. However, this correlation is unusually steep for a black hole X-ray binary: $b \sim 1.4$ (with $L_{\rm radio} \propto L_{\rm X}^{b}$). Below a critical luminosity, the correlation becomes shallower until it rejoins the standard correlation with $b \sim 0.6$. Based on these results, we first show that the steep correlation can be explained if the inner accretion flow is radiatively efficient during the hard state, in contrast to what is usually assumed for black hole X-ray binaries in this spectral state. The transition between the steep and the standard correlation would therefore reflect a change from a radiatively efficient to a radiatively inefficient accretion flow. Finally, we investigate the possibility that the discrepancy between 'outliers' and 'standard' black holes arises from the outflow properties rather than from the accretion flow.

Key words: accretion, accretion discs – ISM: jets and outflows – radio continuum: stars – X-rays: binaries – X-rays: individual: H1743−322.

1 INTRODUCTION

Black hole X-ray binaries (BHXBs) are binary systems consisting of a black hole primary in orbit with a less evolved companion star. These systems spend most of their time in a faint quiescent state, being barely detectable at almost all wavelengths. They may undergo sudden and bright few-month-long X-ray outbursts with typical recurrence periods of many years (Tanaka & Shibazaki 1996). The picture commonly accepted to explain the emission of such objects involves an optically thick and geometrically thin accretion disc, mostly emitting at typical energies of ∼1 keV. This region is probably surrounded by a corona of hot plasma, where ultraviolet (UV) and soft X-ray photons originating from the disc undergo inverse Compton scattering, producing a power-law spectrum in the hard X-ray band. In addition to this 'X-ray picture', BHXBs are also characterized by the intermittent presence of relativistic outflows. This ejected material is mainly detected at radio wavelengths (see e.g. Hjellming & Johnston 1981; Mirabel & Rodriguez 1994; Fender 2006) though it can sometimes dominate the low-frequency emission up to the near-infrared (Corbel et al. 2001; Jain et al. 2001; Corbel & Fender 2002; Homan et al. 2005b; Russell et al. 2006; Coriat et al. 2009). These jets are undoubtedly coupled to the accretion flow, although the nature of this connection is still unclear.

⋆E-mail: m.coriat@soton.ac.uk
†Present address: School of Physics and Astronomy, University of Southampton, Southampton SO17 1BJ.

Several spectral states have been identified based on the relative strengths and properties of the different X-ray emitting components (see e.g. Homan & Belloni 2005; McClintock & Remillard 2006). The two main spectral states are the soft state, dominated by thermal emission from the accretion disc, and the hard state, dominated by emission from the corona. Various instances (hard or soft) of the intermediate state have also been defined to describe the transition phases between the two main states. During these phases the X-ray spectra usually display hardnesses in between those of the hard and the soft state as a result of comparable contributions to the emission from the disc and the corona. These spectral characteristics are also coupled to different levels of X-ray variability (see e.g. van der Klis 2006; Belloni 2010, for a review).

The radio emission in the hard state is usually characterized by a flat or slightly inverted spectrum ($S_\nu \propto \nu^\alpha$ with $\alpha \sim 0$). This is interpreted as self-absorbed synchrotron emission from steady, collimated, compact jets, in analogy with those observed in active galactic nuclei (Blandford & Königl 1979; Hjellming & Johnston 1988). During the soft state these compact jets are thought to be quenched (Fender et al. 1999; Corbel et al. 2000) and any radio emission, if present, is attributed to residual optically thin synchrotron emission from transient ejecta (Corbel et al. 2004; Fender, Belloni & Gallo 2004).

Observations of several sources have provided evidence that a strong connection exists between radio and X-ray emission during the hard state (Hannikainen et al. 1998; Corbel et al. 2000, 2003; Gallo, Fender & Pooley 2003). This connection takes the form of a non-linear flux correlation, $F_{\rm Rad} \propto F_{\rm X}^b$, where $F_{\rm Rad}$ is the radio flux density, $F_{\rm X}$ is the X-ray flux and $b \sim 0.5$–0.7. It was subsequently shown that this same correlation also holds between optical–infrared (OIR) and X-ray fluxes (Homan et al. 2005b; Russell et al. 2006, 2007; Coriat et al. 2009). These correlations indicate that the compact jets are strongly connected with the accretion flow (disc and/or corona), and possibly that their emission (synchrotron and/or inverse Compton) can comprise a significant contribution to the observed high-energy flux (see e.g. Markoff, Falcke & Fender 2001; Markoff et al. 2003; Markoff, Nowak & Wilms 2005; Rodriguez et al. 2008a; Russell et al. 2010). This radio/X-ray correlation, initially established for the source GX 339-4, has been extended to other Galactic black holes (mainly V404 Cyg; Gallo et al. 2003; Corbel, Körding & Kaaret 2008b) and even active galactic nuclei (Merloni, Heinz & di Matteo 2003; Falcke, Körding & Markoff 2004; Körding, Falcke & Corbel 2006a). Migliari & Fender (2006) also showed that a similar correlation exists for neutron star X-ray binaries (NSXBs), but with a steeper correlation coefficient ($b \sim 1.4$) and fainter radio emission for a given X-ray luminosity than seen in black holes (Fender & Hendry 2000; Fender & Kuulkers 2001; Muno et al. 2005).

However, in the following years, a few Galactic black hole candidates (BHCs) were found to lie well outside the scatter of the original radio/X-ray correlation (e.g. XTE J1720−318, Brocksopp et al. 2005; XTE J1650−500, Corbel et al. 2004; IGR J17497−2821, Rodriguez et al. 2007; Swift J1753.5−0127, Cadolle Bel et al. 2007; Soleri et al. 2010), thus either increasing its scatter or challenging the universality of the correlation itself. Some of them could also be false identifications of black holes. For a given X-ray luminosity, these outliers show a radio luminosity fainter than expected from the correlation (thus are sometimes dubbed 'radio-quiet' BHCs). However, for most of these outliers, there are no radio measurements available at low X-ray luminosities. Therefore we do not know whether they remain underluminous in the radio band at low accretion rates. The current lack of data also precludes a precise measurement of the slope of the correlation (if any) for the outliers. It is therefore unclear whether they follow a correlation similar to the 'standard' BHXBs but with a lower normalization or whether their inflow/outflow connection is intrinsically different. Moreover, we do not know if their behaviour is recurrent over several outbursts. These are some of issues that we address in this work.

Note that in the following, we will use the term 'outliers' rather than 'radio-quiet BHCs' to describe these sources. As we will show, they could be considered 'X-ray loud' as well. However, it should be borne in mind that the term 'outliers' might not be appropriate either. Indeed, given the increasing number of these sources, the 'outliers' could in fact turn out to be the norm.

1.1 H1743−322

The X-ray transient H1743−322 was discovered with the *Ariel V* and *HEAO-1* satellites by Kaluzienski & Holt (1977) during a bright outburst in 1977. In 2003, another bright outburst was first detected with the *International Gamma-ray Astrophysics Laboratory* (*INTEGRAL*). The source was initially dubbed IGR J17464−3213, before it was identified as H1743−322 (Markwardt & Swank 2003). This outburst was extensively studied at all wavelengths (see e.g. Parmar et al. 2003; Capitanio et al. 2005; Homan et al. 2005a; Joinet et al. 2005; Lutovinov et al. 2005; Kalemci et al. 2006; Miller et al. 2006; McClintock et al. 2009). It was shown in particular that the spectral and timing features of H1743−322 were similar to those of other, dynamically confirmed, black hole X-ray transients (McClintock et al. 2009). It was thus classified as a BHC.

During the return to quiescence following this outburst, Corbel et al. (2005) reported the detection of large-scale, synchrotron-emitting jets moving away from the central source. These jets were detected at both radio and X-ray wavelengths as a consequence of the interaction between the ejected plasma and the interstellar medium (ISM). Using the observed proper motions of the X-ray jets, these authors also derived an upper limit to the source distance of 10.4 ± 2.9 kpc. Given its location ($l = 357.255$ and $b = -1.83$) in the direction of the Galactic bulge, and a rather high column density, this upper limit is consistent with a Galactic Centre distance for H1743−322. In the following, we will therefore assume a distance of 8 kpc.

The 2003 outburst was followed by weaker outbursts (see Fig. 1) in 2004 (Swank 2004) and 2005 (Rupen, Mioduszewski & Dhawan 2005) which were poorly sampled at both X-ray and radio wavelengths. Therefore, no detailed studies of these two phases have been carried out to date. Further outbursts were observed in the first months of 2008 (2008a in the following; Kalemci et al. 2008; Jonker et al. 2010) and in 2008 September–November (2008b in the following; Corbel et al. 2008a). During the outburst decay of the 2008a outburst, Jonker et al. (2010) reported a radio/X-ray correlation slope of $b = 0.18 \pm 0.01$. The authors also found that H1743−322 lies well below the 'universal' radio/X-ray correlation making of H1743−322 another outlier. The weak 2008b outburst was classified as 'failed'. The source made a short cycle between the hard and the hard intermediate state but never reached the soft state (Capitanio et al. 2009; Prat et al. 2009). The source entered another outburst phase in 2009 (Krimm et al. 2009; Chen et al. 2010) and also in early 2010 (Yamaoka et al. 2009). In 2009, the system followed the canonical evolution through all the characteristic states (Motta, Muñoz-Darias & Belloni 2010). The variation of the flux associated with the two main spectral components (i.e. disc and power law) allowed Motta et al. (2010) to set a lower limit to the orbital inclination of the system of $\geq 43^\circ$.

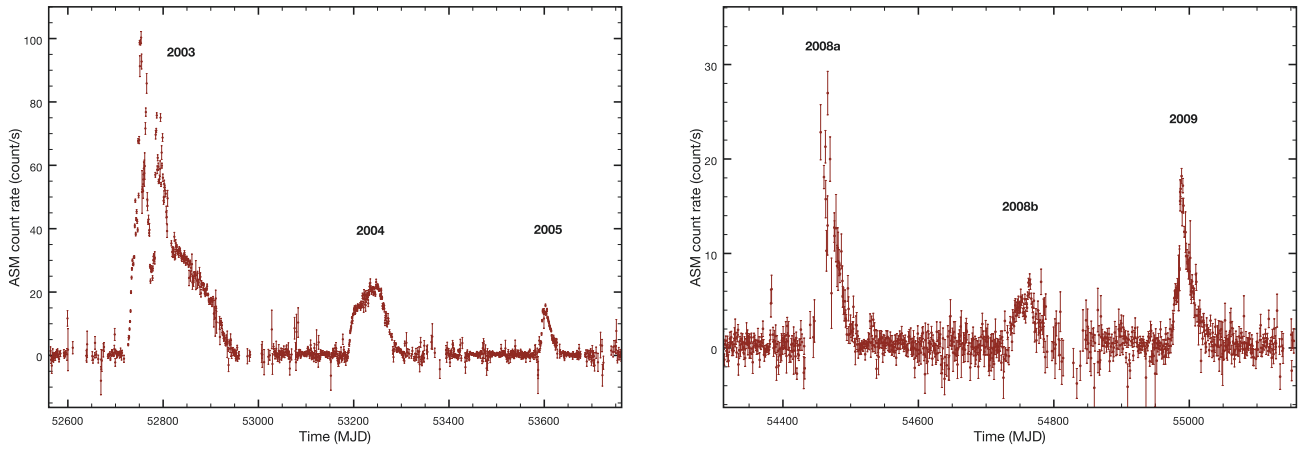

Figure 1. *RXTE*/ASM light curve of H1743−322 between 2003 and 2009. We note a major outburst in 2003 followed by five minor activity periods between 2004 and 2009. Note the different scaling between the two plots. The 2010 light curve is not presented due to the very low number of counts detected by the ASM during this short outburst.

In this work, we focus on the long-term study of the radio/X-ray correlation over the six outbursts mentioned above. We aim to investigate in detail the accretion–ejection coupling in this system in the global context of the 'outliers' of the radio/X-ray correlation. The sequence of observations and data reduction processes is described in Section 2. In Section 3, we present the analysis of the radio/X-ray correlation, the selection process that we applied to isolate and study the connection between the compact jets and the inner accretion flow and finally a comparison with other black hole and neutron star X-ray binaries. These results are then discussed in Section 4, in which we investigate several possible interpretations. Our conclusions are summarized in Section 5.

2 OBSERVATIONS

2.1 X-ray

2.1.1 RXTE: data reduction and spectral analysis

We analysed all publicly available observations of H1743−322 in the *RXTE* archive taken between 2003 January 1 and 2010 February 13. The data were reduced using the HEASOFT software package v6.8, following the standard steps described in the *RXTE* cookbook.[1] Spectra were extracted from the Proportional Counter Array (PCA; Jahoda et al. 2006) in the 3–25 keV range. We only used the top layer of the Proportional Counter Unit (PCU) 2 as it is the only operational unit across all observations and is the best-calibrated detector out of the five PCUs. Systematic errors of 0.5 per cent were added to all channels. In the 20–150 keV range, we used data from the High Energy X-ray Timing Experiment (HEXTE), which we reduced following standard steps. From 2005 December, due to problems in the rocking motion of Cluster A, we extracted spectra from Cluster B only. Because of the low count rate in the HEXTE data in most of the observations, all channels were rebinned by a factor of 4.

In addition, we constructed hardness–intensity diagrams (HIDs) from PCA data. These data were extracted from PCU2 (all layers) and corrected for background. Averaged count rates were extracted in two bands: (standard 2) channels 2–10 and 19–40, corresponding to 2.5–6.1 and 9.4–18.5 keV, respectively. The hardness ratio was defined as the ratio of the flux in the second band to that in the first band, and the intensity was calculated as the sum of the fluxes in both bands. The HIDs are presented in Fig. 2.

We performed a simultaneous fit to the PCA and HEXTE spectra in XSPEC V12.5.1n, using a floating normalization constant to allow for cross-calibration uncertainties. The main objective of the X-ray spectral analysis was to obtain a correct estimation of the unabsorbed flux in the 3–9 keV band. Consequently, we used simple models to reproduce the spectra and achieve statistically acceptable fits (i.e. a reduced $\chi^2 < 2$). We used a power law (*powerlaw*) and an absorption component (*phabs*) as a starting model. When required by an *F* test, we added a multitemperature disc blackbody (*diskbb*) and/or a high-energy cut-off (*highecut*). Eventually, when the residuals indicated the presence of reflection features, we used a Gaussian emission line (*Gaussian*, constrained in energy between 6 and 7 keV) and smeared absorption edge (*smedge*, constrained in energy between 7 and 9 keV). The hydrogen column density was fixed at the value obtained by Prat et al. (2009)[2] using *Swift* and *XMM–Newton* observations, i.e. $N_{\rm H} = 1.8 \pm 0.2 \times 10^{22}$ cm^{-2}. At low count rates, when H1743−322 was not significantly detected by HEXTE, fits were made to the PCA spectrum only. We finally obtained an average reduced χ^2 of 1.04 with a minimum of 0.64 and a maximum of 1.35. Unabsorbed fluxes were then estimated in the 3–9 keV energy ranges, according to the PCA normalization.

Because of the location of the source close to the Galactic plane, the Galactic ridge emission starts to significantly contaminate the estimated 3–9 keV PCA flux below $\sim 10^{-10}$ erg s^{-1} cm^{-2}. Kalemci et al. (2006) determined a 3–25 keV unabsorbed flux from the ridge emission of 1.08×10^{-10} erg s^{-1} cm^{-2}, based on the analysis of nine observations in 2004 (MJD 53021–53055). We analysed the same data set to estimate the ridge emission in the 3–9 keV band and found an unabsorbed flux of $(6.0 \pm 0.6) \times 10^{-11}$ erg s^{-1} cm^{-2}. Consequently, we subtracted this value from all 3–9 keV PCA fluxes. To

[1] http://heasarc.gsfc.nasa.gov/docs/xte/data_analysis.html

[2] Note that several estimates of the hydrogen column density are found in the literature. The values range from 1.6×10^{22} (e.g. Capitanio et al. 2009) to 2.3×10^{22} cm^{-2} (e.g. Miller et al. 2006). However, within this range, the precise value of the $N_{\rm H}$ and its possible variation during the outburst has little influence on the unabsorbed flux above 3 keV. We thus used the intermediate value found by Prat et al. (2009).

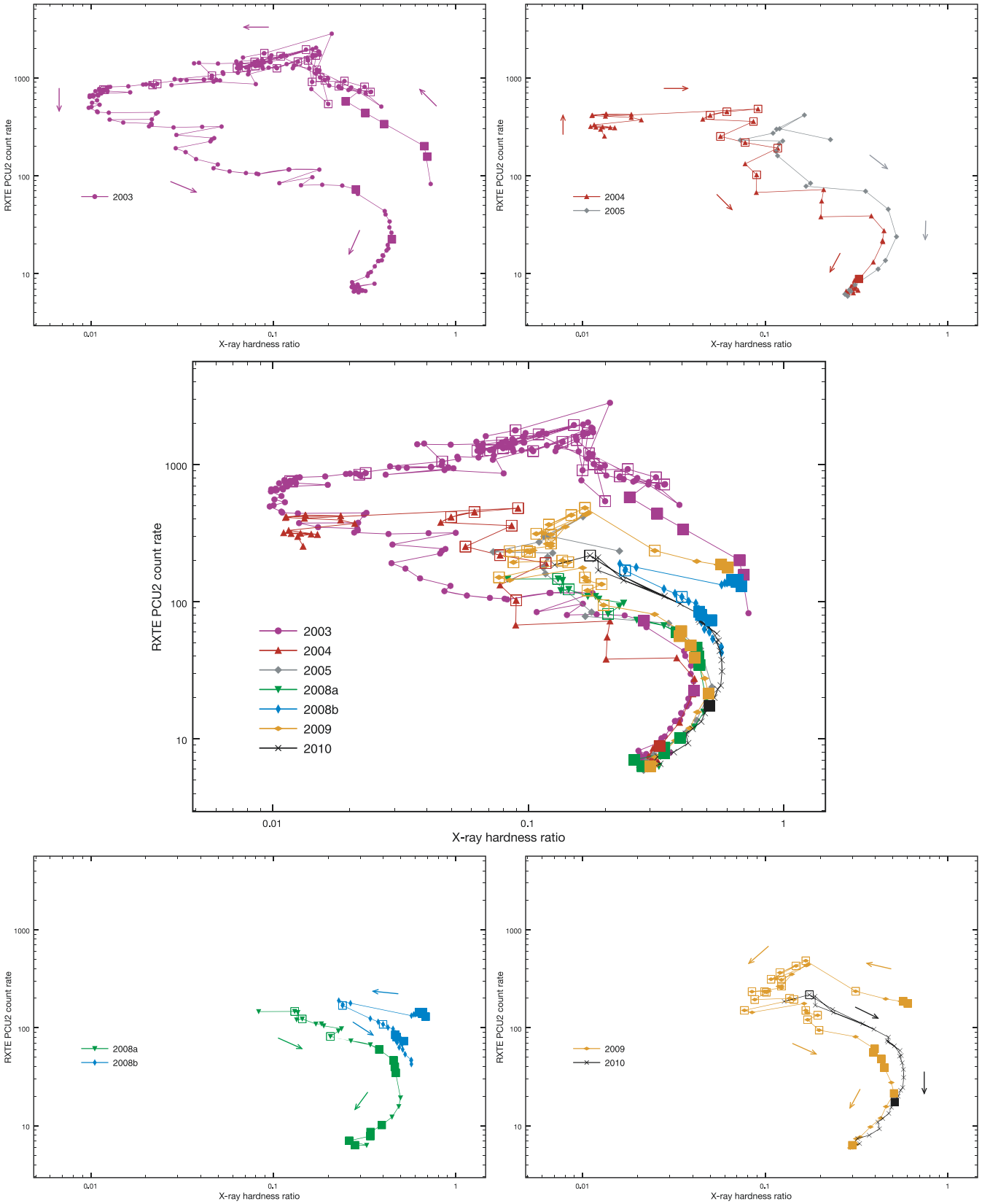

Figure 2. HIDs of H1743−322 from 2003 to 2010. Squares (open and filled) indicate the radio detections, plotted on top of the HIDs at the location of the nearest *RXTE* observation. Filled squares indicate the data selected for the radio/X-ray diagram in Fig. 4. The radio and X-ray fluxes corresponding to this selection are detailed in Table 1. Arrows indicate the temporal evolution during the outbursts. X-ray observations are indicated by purple circles for the outburst in 2003, red triangles for 2004, grey diamonds for 2005, inverted green triangles for 2008a, blue diamonds for 2008b, orange lozenges for 2009 and black crosses for 2010.

check whether a simple subtraction was appropriate to correct the measured source flux for the contamination from the ridge emission, we combined the spectra of the nine observations mentioned above to obtain a typical ridge spectrum. We then used this as an additional background spectrum for several on-source observations, where the ridge emission made a significant contribution. Finally, we compared the 3–9 keV fluxes obtained using this method with those obtained via simple flux subtraction. There was no significant difference within the error bars.

2.1.2 Other X-ray satellites

Jonker et al. (2010) studied the decay of the 2008a outburst using *Chandra* and *Swift* X-ray data simultaneous with radio observations from the Very Large Array (VLA). Since they provide important constraints on the correlation at low luminosity, we included in our study the X-ray fluxes published in their paper. We converted the unabsorbed 0.5–10 keV fluxes into absorbed 3–9 keV fluxes with the WEBPIMMS tool[3] using the $N_{\rm H}$ and photon index provided by the authors. For consistency with the *RXTE* data, we then calculated the unabsorbed 3–9 keV fluxes using $N_{\rm H} = 1.8 \times 10^{22}$ cm^{-2}.

2.1.3 X-ray state classification

Since the definition and nature of the X-ray states is still debated, in the following, we will adopt a simplified classification adapted to the purpose of this work. Our aim is to understand the nature of the connection between the corona and the compact jets for the outliers of the radio/X-ray correlation. Therefore, we will be mainly interested in phases where the compact jets are present and where the X-ray emission in the 3–9 keV band is dominated by the power-law emitting component. Consequently, we will define only three states: hard, soft and intermediate. To be classified as hard state, we require that the power-law component dominates the X-ray spectrum in the sense that an accretion disc component was not required (by an *F* test) to correctly fit the data above 3 keV. We also require a power-law photon index $\Gamma < 2$. We define the soft state by a power-law photon index $\Gamma > 2$ and a disc flux comprising >75 per cent of the 3–9 keV flux. All observations that do not correspond to either of these criteria are classified as intermediate states.

2.2 Radio

2.2.1 ATCA

Between 2003 April 24 (MJD 52753) and 2010 February 13 (MJD 55240), we performed a total of 38 observations of H1743−322 with the Australia Telescope Compact Array (ATCA). From 2009 April, the observations were carried out using the Compact Array Broadband Backend (CABB). This upgrade has provided a new broad-band backend system for the ATCA, increasing the maximum bandwidth from 128 MHz to 2 GHz. Each observation was conducted simultaneously in two different frequency bands, with central frequencies of 4.8 and 8.64 GHz (5.5 and 9 GHz, respectively, following the CABB upgrade). Various array configurations were used during these observations.

The ATCA has orthogonal linearly polarized feeds and full Stokes parameters (*I*, *Q*, *U*, *V*) are recorded at each frequency. We used PKS 1934−638 for absolute flux and bandpass calibration, and PMN 1729−37 to calibrate the antenna gains and phases as a function of time. We determined the polarization leakages using either the primary or the secondary calibrator, depending on the parallactic angle coverage of the secondary. Imaging was carried out using a combination of multifrequency (Sault & Wieringa 1994) clean and standard clean algorithms. The editing, calibration, Fourier transformation, deconvolution and image analysis were carried out with the Multichannel Image Reconstruction, Image Analysis and Display (MIRIAD) software (Sault, Teuben & Wright 1995).

2.2.2 VLA

H1743−322 has also been regularly observed between 2003 and 2010 with the VLA. To extend our data set, we made use of the radio flux densities at 4.86 and 8.46 GHz published in McClintock et al. (2009) for the 2003 outburst, in Rupen, Mioduszewski & Dhawan (2004) and Rupen et al. (2005) for the 2004 and 2005 outbursts and in Rupen, Dhawan & Mioduszewski (2008a,b) and Jonker et al. (2010) for the 2008a outbursts. We collected a total of 68 VLA pointings. All VLA data are summarized in the aforementioned references in which data reduction and analysis are detailed. In addition, we retrieved unpublished archival data of the 2004 outburst (PI: Rupen) from the National Radio Astronomy Observatory (NRAO) data base. All data were reduced using standard procedures within the NRAO AIPS software package, using 3C 286 as our primary calibrator, and J1744−3116 as the secondary calibrator.

For the 2009 outburst, we triggered VLA observations of H1743−322 after detection of an X-ray flare by *Swift*/Burst Alert Telescope (BAT) on 2009 May 26 (Krimm et al. 2009). On 2009 May 27, we detected unresolved radio emission at 8.4 GHz and triggered a monitoring campaign to cover the outburst of the source from the rising hard state through the decay back to quiescence. Our final observation was taken on 2009 August 6. Observations were made in dual circular polarization in each of two contiguous intermediate frequency pairs, giving a total bandwidth of 100 MHz per polarization. We observed primarily at 8.4 and 4.8 GHz, but also at 1.4 GHz when the source flux density was predicted to be above 0.3 mJy, and at 22.4 GHz for two epochs at the peak of the flare, although the source was not detected in either observation at this frequency. The array was in its intermediate CnB and C configurations throughout the duration of our observing campaign.

2.3 Simultaneity

For the vast majority of the radio data, we found quasi-simultaneous ($\Delta t \leq 1$ d) *RXTE* observations. Otherwise, we interpolated the X-ray flux from a polynomial fit to the PCA light curve. We estimated that the uncertainty introduced by this method should be less than 15 per cent as the flux evolution was found to be smooth in all cases. When the missing flux was not framed by at least two X-ray pointings, we converted the *RXTE*/All Sky Monitor (ASM) count rate into 3–9 keV unabsorbed flux with WEBPIMMS, using the spectral parameters of the nearest X-ray observation.

3 RADIO/X-RAY CORRELATION

3.1 Overview

In a first approach to characterize the global radio-X-ray behaviour of H1743−322, we use the complete data set without restricting

[3] http://heasarc.gsfc.nasa.gov/Tools/w3pimms.html

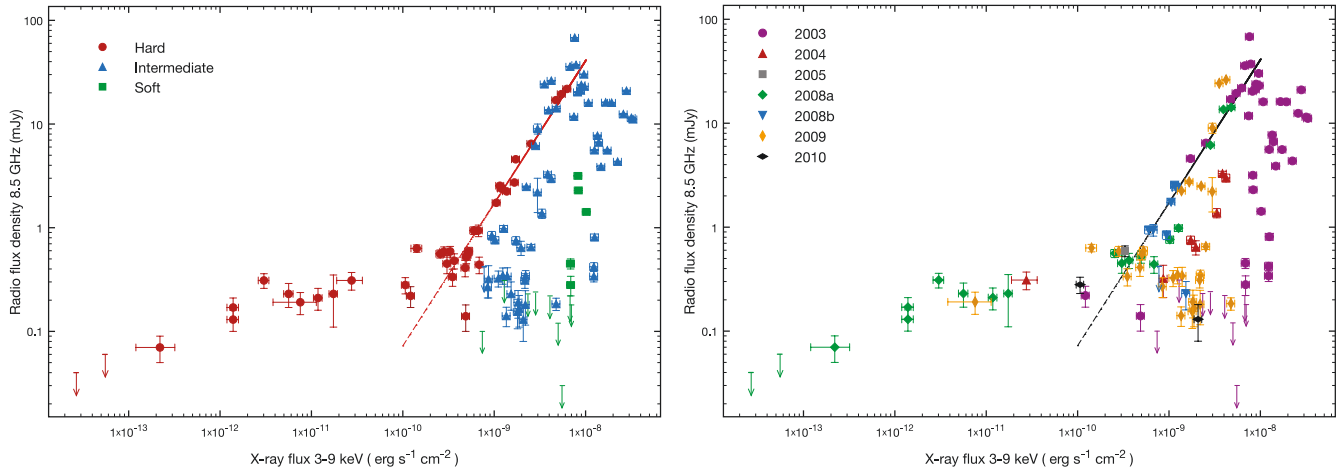

Figure 3. Quasi-simultaneous 8.5 GHz radio flux density versus 3–9 keV X-ray flux during the seven outbursts. (a) Left-hand panel: data are colour coded according to X-ray state. Red circles, green squares and blue triangles indicate the hard, soft and intermediate state, respectively. Dashed line indicates the power-law fit to the selected hard state data (see Section 3.2). (b) Right-hand panel: same as left-hand panel but with the colour code indicating the outburst, as labelled in the figure legend.

either the X-ray state or the origin of the radio emission (e.g. compact jet, discrete ejecta, interaction with the ISM). Fig. 3 shows the 8.5 GHz radio flux density[4] versus the 3–9 keV unabsorbed flux over the 2003, 2004, 2005, 2008a, 2008b, 2009 and 2010 outbursts. The left-hand panel of Fig. 3 shows the data grouped according to the X-ray state. The right-hand panel shows the data grouped by outburst.

3.1.1 Behaviour at high flux

Above a 3–9 keV X-ray flux $\sim 2 \times 10^{-10}$ erg s^{-1} cm^{-2}, the behaviour of H1743−322 seems compatible, on first inspection, with the radio/X-ray behaviour typically observed during an outburst of a BHXB (for a detailed discussion on this unified picture see e.g. Fender, Homan & Belloni 2009 and references therein). The hard state shows correlated radio and X-ray emissions over two orders of magnitude in radio flux density. On average, it is the most radio loud state for a given X-ray luminosity. During the intermediate state, the X-ray emission increases but is not correlated with the radio emission. For most of the radio observations during the intermediate state, the spectral index is indicative of optically thin synchrotron emission from transient ejecta ($\alpha \lesssim -0.5$, where radio flux density S_ν scales with frequency ν as $S_\nu \propto \nu^\alpha$). During the soft state, the radio emission is usually not detected as illustrated by the upper limits, however, we note several radio detections during the soft state of the 2003 outburst. This residual emission shows optically thin spectra and could originate from the interaction of the ejected matter with the environment, as was later observed on larger scales (Corbel et al. 2005).

3.1.2 Behaviour at low flux

If we consider now the entire plot including the low flux data, we note several data points that clearly depart from the main hard state correlation below $\sim 2 \times 10^{-10}$ erg s^{-1} cm^{-2} in the 3–9 keV X-ray band. Most of these points (green diamonds in Fig. 3b) belong to the decay phase of the 2008a outburst and were obtained using the *Chandra* and *Swift* satellites along with the VLA (Jonker et al. 2010). The origin of the radio emission is unclear since most of the VLA observations were conducted at only one frequency. For three of them, however, upper limits at 1.4 GHz are available. The corresponding lower limits on the radio spectral indices ($\alpha \geq -0.58$, -0.53 and -0.60) encompass both possibilities of optically thick and thin spectra. On the other hand, we note that the data from the declining hard state of the 2004 and 2009 outbursts (and possibly also 2003 and 2010) also deviate from the main correlation and seem to follow the same trend as the 2008a data. Moreover, their nearly flat radio spectra are consistent with a compact jet origin. This would suggest that this deviation is a significant evolution of the inflow–outflow connection when the source reaches low luminosities.

3.1.3 Jet quenching factor

The drop in radio flux density during the hard to soft state transition is usually attributed to the quenching of the compact (core) jets. To estimate the level of this suppression, we can use the ratio between the highest radio flux attributed to compact jet emission from the initial hard state of an outburst, and the lowest radio upper limit obtained during the soft state of the same outburst. The 3σ upper limit of 0.03 mJy obtained on MJD 52863 during the soft state of the 2003 outburst, provides a quenching factor of $\sim$700, which is, as far as we know, the strongest constraint to date (Fender et al. 1999; Corbel et al. 2001, 2004) supporting the idea of jet suppression during the soft state.

3.2 Isolating the compact jet–corona connection

The radio/X-ray correlation in BHXBs is usually observed during the canonical hard state where the radio and X-ray emission are assumed to originate from the compact jets and the corona, respectively. To study this connection in detail, we restricted our data set to observations in the hard state for which the radio spectrum was indicative of optically thick synchrotron emission from compact jets, i.e. a radio spectral index whose lower limit is ≥ -0.3. We also

[4] We use an average frequency of 8.5 GHz for simplicity since the radio data come from the VLA (8.46 GHz) and the ATCA (8.64 GHz). Even for an optically thin spectrum with spectral index $\alpha = -0.6$, the effect of this simplification would be <1.5 per cent.

discarded observations that took place following the first radio flare of an outburst, since the compact jets might be disrupted when discrete ejection events take place (see e.g. Corbel et al. 2004; Fender et al. 2004, 2009).

The selected radio and X-ray fluxes are summarized in Table 1 and the radio/X-ray plot obtained using these filtered data is shown in Fig. 4. Above $\sim 2 \times 10^{-10}$ erg s^{-1} cm^{-2} in the 3–9 keV X-ray band, we note a clear correlation over almost two orders of magnitude in radio flux density. We fit the data with a power-law function of the form $F_{\rm Rad} = k F_{\rm X}^{b}$, where $F_{\rm Rad}$ is the radio flux density at 8.5 GHz (in mJy) and $F_{\rm X}$ is the unabsorbed 3–9 keV X-ray flux (in erg s^{-1} cm^{-2}). We obtain a correlation index $b = 1.38 \pm 0.03$ and a normalization constant $k = 4.43 \times 10^{12}$ mJy erg^{-1} s cm^{2}. The correlation index $b \sim 1.4$ clearly differs from the range of values ($b \sim 0.5$–0.7) observed for other BHXBs (e.g. GX 339-4, V404 Cyg, XTE J1118+480; see Corbel et al. 2003, 2008b; Gallo et al. 2003; Xue & Cui 2007). Interestingly, it corresponds to the correlation index found for atoll source neutron stars in the island state (Migliari & Fender 2006), a state that shares similar properties with the hard state of BHXBs. We also note that our derived correlation index is not consistent with the one found by Jonker et al. (2010), i.e. $b = 0.18 \pm 0.01$. However, this index is obtained by fitting the low-luminosity data of the 2008a outburst. Our work suggests that this low value likely reflects a transition phase (see Section 3.3).

We note however that it is the high-flux data from 2003 that mostly constrain the correlation index since it is the brightest outburst observed to date from H1743−322. None the less, if we exclude the 2003 data from the fitting process, we obtain the following

Table 1. X-ray fluxes and radio flux densities selected for the correlation presented in Fig. 4. Unless otherwise stated, the X-ray data are from the *RXTE*-PCA instrument. All *RXTE* fluxes are corrected for the Galactic ridge emission. We also indicate the interferometer used for the radio observations.

Calendar date	MJD	X-ray 3–9 keV unabs. flux (10^{-11} erg s^{-1} cm^{-2})	Radio 8.5 GHz flux density (mJy)	Notes
2003 March 30	52728.59	172 ± 20	4.57 ± 0.12	VLA (1,A)
2003 April 01	52730.55	253 ± 1	6.45 ± 0.12	VLA (1)
2003 April 03	52732.55	474 ± 50	16.99 ± 0.12	VLA (1,B)
2003 April 04	52733.55	626 ± 2	21.81 ± 0.13	VLA (1)
2003 April 06	52735.47	545 ± 7	19.43 ± 0.16	VLA (1)
2003 November 05	52948.00	12.16 ± 0.91	0.22 ± 0.05	VLA (1)
2004 November 01	53310.87	2.75 ± 0.86	0.31 ± 0.06	ATCA
2005 August 07	53589.25	33.0 ± 1.5	0.59 ± 0.07	VLA (2,A)
2008 January 28	54493.32	68.5 ± 5.3	0.44 ± 0.09	ATCA
2008 February 03	54499.74	49.5 ± 3.6	0.52 ± 0.07	VLA (3)
2008 February 05	54501.64	36.5 ± 4	0.48 ± 0.08	VLA (3)
2008 February 06	54502.56	30.424 ± 3	0.45 ± 0.09	VLA (3)
2008 February 09	54505.67	25.60 ± 3	0.56 ± 0.05	VLA (3)
2008 February 19	54515.63	1.74 ± 0.25	0.23 ± 0.12	*Swift* – VLA (3,4)
2008 February 20	54516.55	1.18 ± 0.3	0.21 ± 0.05	*Chandra* – VLA (3,4)
2008 February 23	54519.69	0.56 ± 0.06	0.23 ± 0.06	*Chandra* – VLA (3,4)
2008 February 24	54520.69	0.30 ± 0.04	0.31 ± 0.05	*Swift* – VLA (3,4)
2008 March 01	54526.59	0.14 ± 0.02	0.17 ± 0.04	*Chandra* – VLA (3,4)
2008 March 02	54527.53	0.14 ± 0.02	0.13 ± 0.03	*Chandra* – VLA (3,4)
2008 March 08	54533.56	0.022 ± 0.01	0.07 ± 0.02	*Chandra* – VLA (3,4)
2008 October 05	54744.21	105 ± 14	1.74 ± 0.07	ATCA
2008 October 08	54747.44	115 ± 2	2.54 ± 0.08	ATCA
2008 October 09	54748.44	119 ± 2	2.43 ± 0.09	ATCA
2008 October 10	54749.36	121 ± 3	2.38 ± 0.11	ATCA
2008 November 04	54774.43	67.3 ± 2.5	0.94 ± 0.12	ATCA
2008 November 09	54779.35	60.1 ± 1.9	0.94 ± 0.08	ATCA
2009 May 27	54978.38	137 ± 14	2.24 ± 0.03	VLA (A)
2009 May 30	54981.95	166 ± 7	2.73 ± 0.10	VLA
2009 July 07	55019.46	52.8 ± 5.8	0.592 ± 0.055	VLA
2009 July 08	55020.30	50.7 ± 5	0.546 ± 0.06	VLA (B)
2009 July 09	55021.42	48.1 ± 5.3	0.41 ± 0.074	VLA
2009 July 12	55024.28	35.0 ± 3	0.335 ± 0.063	VLA (B)
2009 July 13	55025.28	28.2 ± 1.9	0.587 ± 0.066	VLA
2009 July 19	55031.29	14.2 ± 1.9	0.631 ± 0.052	VLA
2009 August 06	55049.60	0.76 ± 0.38	0.191 ± 0.046	VLA
2010 February 13	55240.01	10.6 ± 0.9	0.28 ± 0.05	ATCA

Note. (1) VLA flux density from McClintock et al. (2009); (2) VLA flux density from Rupen et al. (2005); (3) VLA flux density from Jonker et al. (2010); (4) *Swift* and *Chandra* fluxes from Jonker et al. (2010) (see Section 2.1.2);
(A) ASM count rate converted into 3–9 keV unabsorbed flux using WEBPIMMS (see Section 2.3); (B) X-ray flux obtained by interpolation of the PCA light curve (see Section 2.3).

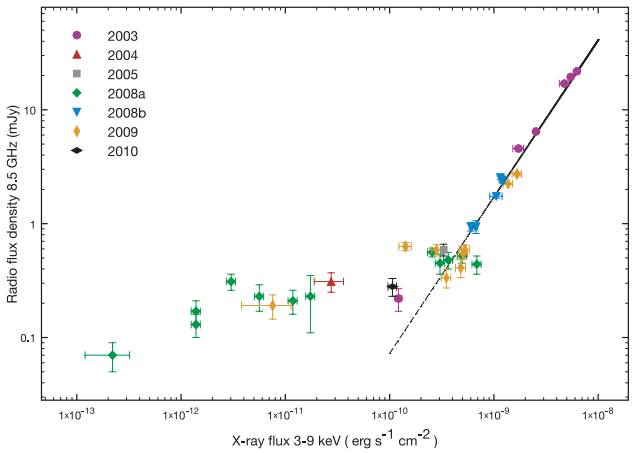

Figure 4. Radio flux density at 8.5 GHz versus the unabsorbed 3–9 keV X-ray flux. This plot shows the data set restrained to the 'canonical' hard state where the radio emission can be attributed to partially self-absorbed synchrotron emission from the compact jets and where the X-ray spectra are dominated by the power-law component. Dashed line indicates the fit to the data above 2×10^{-10} erg s^{-1} cm^{-2} with a function of the form $F_{\rm Rad} = k\, F_{\rm X}^{b}$, with $b = 1.38 \pm 0.03$ and $k = 4.43 \times 10^{12}$ mJy erg^{-1} s cm^{2}.

99.99 per cent confidence interval for the correlation index: [1.19, 1.65]. This remains in good agreement with the previous results and seems to favour a constant slope for all outbursts.

3.3 Comparison with the 'standard' radio/X-ray correlation

To compare the relationship between radio and X-ray fluxes in H1743−322 with the standard radio/X-ray correlation of black hole and neutron star X-ray binaries, we plot in Fig. 5 the hard state data from H1743−322, GX 339-4 (the data cover seven outbursts over the period 1997–2010 and will be detailed in Corbel et al., in preparation), V404 Cyg (Gallo et al. 2003; Corbel et al. 2008b) and the atoll neutron stars Aql X-1 (Tudose et al. 2009; Miller-Jones et al. 2010) and 4U 1728−34 (Migliari & Fender 2006) in the island state. To convert fluxes into luminosity, we used a distance of 8 kpc for GX 339-4 (Zdziarski et al. 2004) and the new distance of 2.39 kpc for V404 Cyg, that was derived using accurate astrometric very long baseline interferometry (VLBI) observations (Miller-Jones et al. 2009). For the neutron stars, we used 5.2 kpc for Aql X-1 (Jonker & Nelemans 2004) and 4.6 kpc for 4U 1728−34 (Galloway et al. 2003).

Fig. 5 shows that for intermediate luminosities ($\sim 10^{36-37}$ erg s^{-1}), H1743−322 lies significantly below the 'standard' correlation for BHXBs but is not compatible either with the neutron star relation. In addition, the figure shows that the deviant points at low luminosity seem to rejoin the standard correlation and then follow it below 2×10^{34} erg s^{-1}. The data points between 2×10^{34} and 2×10^{36} erg s^{-1} seem thus to reflect a transition between the correlation of slope $b = 1.4$ and the standard correlation of slope $b = 0.6$. This supports the idea of a significant change in the coupling between the jets and the corona in H1743−322 when the source reaches low accretion rates.

This transition can be crudely fit with a power-law function with index $b = 0.23 \pm 0.07$ between the 3–9 keV luminosities 2×10^{34} and 2×10^{36} erg s^{-1}. The corresponding bolometric (3–100 keV) luminosities in Eddington units are $L_{\rm stand} \sim 5 \times 10^{-5} L_{\rm Edd}$ and $L_{\rm trans} \sim 5 \times 10^{-3} L_{\rm Edd}$ for a 10 $M_{\odot}$ black hole.

As mentioned in the Introduction, H1743−322 is identified as an outlier of the standard radio/X-ray correlation, as confirmed by

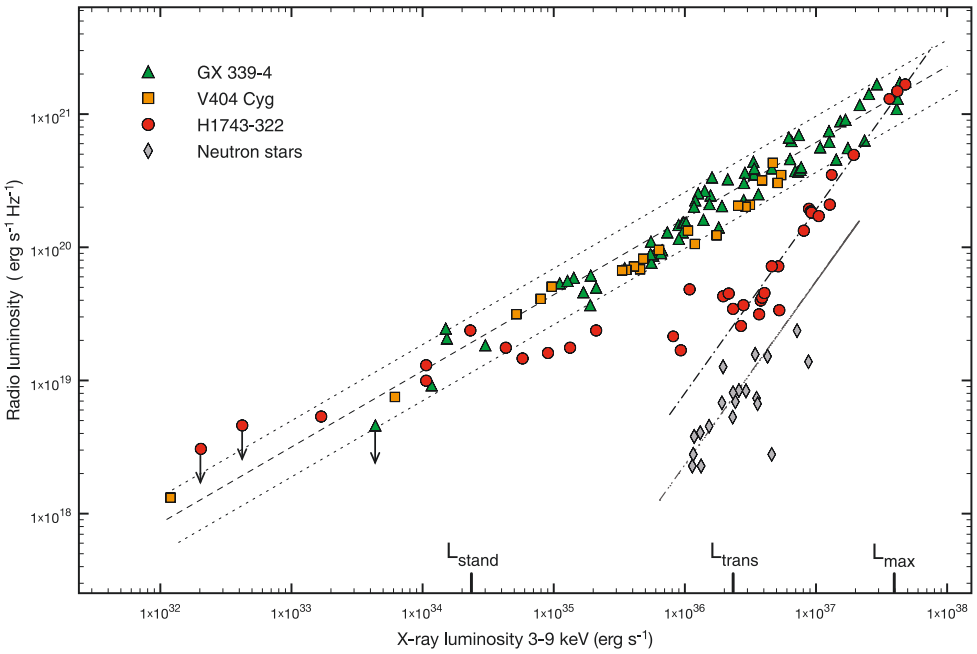

Figure 5. 8.5 GHz radio luminosity against 3–9 keV X-ray luminosity for the BHCs H1743−322, GX 339−4 and V404 Cyg in the hard state. For comparison, we also plot the data from the atoll neutron stars Aql X-1 and 4U 1728−34 in the island state. The dashed line indicates the fit to the GX 339-4 and V404 Cyg data with a relation of the form $L_{\rm radio} \propto L_{\rm X}^{b}$ with a correlation index $b \sim 0.6$. The two dotted lines demarcate the dispersion around the correlation. The dashed–dotted and dashed–dotted–dotted lines indicate the fit to the high-luminosity data of H1743−322 and the neutron star data, respectively, with a correlation index $b \sim 1.4$. On the x-axis, we also indicate three characteristic X-ray luminosities that will ease the discussion. $L_{\rm stand}$ and $L_{\rm trans}$ are, respectively, the lower and the upper bound of the transition between the two correlations. $L_{\rm max}$ indicates the point where the steep correlation of H1743−322 connects to the 'standard' correlation at high luminosity. Note that these three luminosities are defined in the 3–100 keV band in the text.

our results. Some of the numerous questions associated with this outlier population of sources are whether they follow the same correlation slope as the other BHXBs but with a lower normalization, and whether they remain below the standard correlation at low and high luminosity. In the case of H1743−322, we obtain a correlation index of $b = 1.38 \pm 0.03$. This is the first precise measurement of the radio/X-ray correlation of an outlier. If H1743−322 is representative of these 'radio-quiet' Galactic black holes, our results suggest that their location below the 'standard' correlation is a consequence of an intrinsically different coupling between the jets and the corona rather than just a variation of normalization. In this respect, we point out the recent work by Soleri et al. (2010) on the outlier Swift J1753.5−0127. These authors report a slope of the radio/X-ray correlation of the source lying between 1.0 and 1.4, in good agreement with our results on H1743−322. Finally, our results suggest that at high ($\sim L_{\rm max}$) and low luminosity ($\leq L_{\rm stand}$), the outliers might not remain below the standard correlation if they follow the same behaviour as H1743−322 (see Fig. 5).

4 DISCUSSION

4.1 Nature of the compact object

As mentioned above, the mass of the compact object is not yet constrained, so its nature is still uncertain. Based on the radio/X-ray correlation alone and considering the results of Migliari & Fender (2006), the 1.4 power-law index could suggest that the accreting compact object is a neutron star. However and more tellingly, the overall behaviour of the source during an outburst, and its X-ray spectral and timing features are very similar to other, dynamically confirmed, black hole binaries (e.g. XTE J1550−564; McClintock et al. 2009). The source is thus more likely to be a black hole than a neutron star. In the following discussion, we will therefore consider it as such, but note the caveat that a neutron star primary cannot be entirely ruled out.

4.2 Radio-quiet or X-ray-loud microquasar?

As shown in Fig. 5, H1743−322 spans the same range of X-ray and radio luminosity in the hard state as 'standard' microquasars. Consequently, should we consider that it displays dimmer radio emission for a given X-ray luminosity or the contrary? In other words, are we facing a radio-quiet or an X-ray-loud microquasar? In the following, we investigate both hypotheses. First (Section 4.3), we consider that the outliers have a more radiatively efficient X-ray emitting component than the 'standard' microquasars (X-ray loud hypothesis). Then (Section 4.4), we consider that the discrepancy between the two populations of sources arise from different jet properties (radiative efficiency, injected power etc.) leading the outliers to produce fainter radio emission.

4.3 Radiatively efficient accretion flow in the hard state: the X-ray loud hypothesis

We usually define two general classes of accretion flow, depending on whether the gravitational energy of the accreted matter is preferentially released through radiation (radiatively efficient) or carried away with the flow (radiatively inefficient).

Radiatively efficient flows include, for instance, the standard optically thick and geometrically thin accretion disc model (Shakura & Sunyaev 1973), some models of accretion disc coronae (ADC; see e.g. Galeev, Rosner & Vaiana 1979; Haardt & Maraschi 1991; Di Matteo, Celotti & Fabian 1999; Merloni & Fabian 2002) or the luminous hot accretion flow (LHAF) model (Yuan 2001). From simple physical assumptions, the scaling of the X-ray luminosity with accretion rate, in most radiatively efficient flows, is expected to be linear, $L_{\rm X} \propto \dot{M}$.

Radiatively inefficient flows are expected to produce X-ray emission with $L_{\rm X} \propto \dot{M}^{2-3}$. This is the case of accretion flows dominated by advection in which a significant fraction of the energy is advected instead of radiated away. This advected energy can either cross the event horizon [advection-dominated accretion flow (ADAF); Ichimaru 1977; Narayan & Yi 1994; Abramowicz et al. 1996] and/or be expelled in outflows [advection-dominated inflow–outflow solution (ADIOS); Blandford & Begelman 1999]. In such models, the X-ray emission arises mainly from Compton up-scattering of internal (synchrotron, bremsstrahlung) or external (blackbody emission from outer thin disc) photon fields. A similar relation ($L_{\rm X} \propto \dot{M}^{2-3}$) is also obtained in systems dominated by jet emission, where most of the energy is channelled into the jets (Markoff et al. 2003, 2005). The X-rays, in that case, can originate at the base of the jets as optically thin synchrotron emission and/or inverse Compton scattering by the outflowing particles of the jet synchrotron photons [synchrotron self-Compton (SSC)] and disc photons (external Compton).

We will now show that if we assume the standard emission model of compact jets is valid for the outliers, the steep radio/X-ray correlation we have found implies that the accretion flow is radiatively efficient in the hard state, in contrast to what is usually assumed for BHXBs in this X-ray state.

Let us thus consider the classical assumption stating that the total jet power $Q_{\rm jet}$ is a fraction $f_{\rm j} < 1$ of the (maximal) accretion power $Q_{\rm accr}$:

$$Q_{\rm accr} = \dot{M}c^2 \qquad \text{and} \qquad Q_{\rm jet} = f_{\rm j}\, Q_{\rm accr}. \tag{1}$$

The fraction $f_{\rm j}$ is usually considered as constant or at least independent of the accretion rate (see e.g. Blandford & Königl 1979; Falcke & Biermann 1995; Heinz & Sunyaev 2003). $Q_{\rm jet}$ should therefore scale linearly with $\dot{M}$. Since we restrict ourselves to the standard jet emission model, we will adopt this assumption. However, there is no strong physical argument justifying that $f_{\rm j}$ is independent of $\dot{M}$, so we shall discuss it in the next section about the radio-quiet hypothesis.

From the standard equations for synchrotron emission (e.g. Rybicki & Lightman 1979), one can obtain the following scaling between the jet luminosity L_ν at a given frequency and the jet power (see e.g. Heinz & Sunyaev 2003):

$$L_\nu \propto Q_{\rm jet}^{\xi} \qquad \text{with} \qquad \xi = \frac{2p - (p+6)\alpha + 13}{2(p+4)}, \tag{2}$$

and where α is the spectral index of the jet spectrum (with the convention $L_\nu \propto \nu^\alpha$). This relation is valid under the assumptions of the standard model, i.e. a conical jet with an initial energy distribution of relativistic electrons in the form of a power law with index p (for the impact of different assumptions see e.g. Pe'er & Casella 2009). The classical values assumed for p are in the range 2–3 (see e.g. Bell 1978; Blandford & Ostriker 1978; Drury, Axford & Summers 1982; Gallant, Achterberg & Kirk 1999; Achterberg et al. 2001), while the spectral index α of the compact jets in the radio range is usually observed between −0.2 and 0.2. Fig. 6 shows the variation of the exponent ξ as a function of p for different values of α. We note that for the fiducial values of p and α, ξ varies between 1.22 and 1.58 with an average value of $\sim$1.4.

If the observing frequency is located in the radio range, equations (1) and (2) give $L_{\rm radio} \propto \dot{M}^{\xi}$. If we assume that the X-ray luminosity

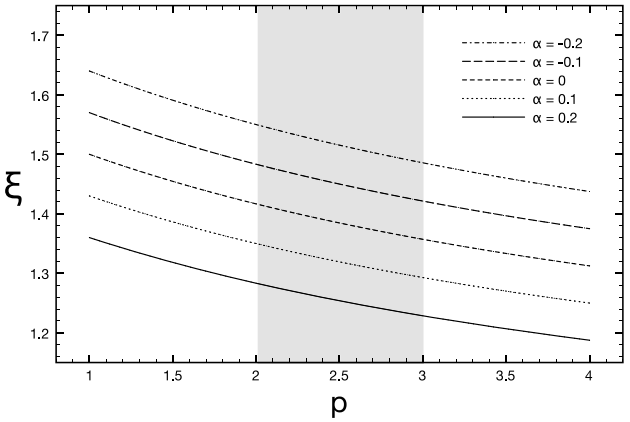

Figure 6. Variation of the exponent ξ in the relation $L_\nu \propto Q_{\rm jet}^{\xi}$, as a function of the power-law index p of the electron distribution, for several values of the spectral index α of the compact jets. Grey zone delimits the range of values usually assumed for the power-law index p.

in the hard state can be written in a general way as $L_{\rm X} \propto \dot{M}^q$, we expect the following relation between radio and X-ray luminosities:

$$L_{\rm radio} \propto L_{\rm X}^{\xi/q}. \quad (3)$$

Consequently, for ξ between 1.22 and 1.58, the radio/X-ray correlation usually found for microquasars ($L_{\rm radio} \propto L_{\rm X}^{0.5-0.7}$), requires $q \sim 2$–3 and thus a radiatively inefficient accretion flow. On the other hand, the $L_{\rm radio} \propto L_{\rm X}^{1.4}$ relation of H1743−322 implies $q \sim 1$, which suggests the X-ray emission in the hard state is produced by a radiatively efficient flow. In this respect, we note that a radiatively efficient flow during the hard state of Cyg X-1 has been found by Malzac, Belmont & Fabian (2009). Moreover, Rushton et al. (2010) have shown that GRS 1915+105 could be radiatively efficient during its plateau state. This in turn would be consistent with the fact that it lies on the extension, at high luminosity, of the correlation of H1743−322 (Coriat et al. 2011).

As mentioned previously, to obtain the radio/X-ray plot in Fig. 4, we filtered the X-ray data to minimize the thermal contribution of the thin disc. We can thus exclude the possibility that the disc contaminates the 3–9 keV emission enough to produce the observed correlation.

As far as we know, besides the standard accretion disc solution, the other models of radiatively efficient accretion flows can be divided in two categories according to their geometry.

(i) Hot accretion flow: the standard accretion disc extends to a truncation radius, where it is replaced by a hot and geometrically thick flow in the inner parts.

(ii) ADC: the standard accretion disc extends close to the black hole and is 'sandwiched' by a corona of hot plasma.

In both categories, several models have been developed to explain the properties of BHXBs in the hard state by coupling the accretion flow with steady jets. While the aim of this work is not to review all these models, we briefly examine some examples below.

4.3.1 Hot accretion flows

Most hot accretion flow models are found to be radiatively inefficient, at least at low accretion rates (e.g. ADAF, ADIOS, CDAF), and can only exist below a critical accretion rate ($\sim 10^{-1}$–$10^{-2}(L_{\rm Edd}/c^2)$). However, Yuan (2001) has shown that a hot flow may be maintained above the critical accretion rate when Coulomb coupling between electrons and ions becomes more effective due to increasing density. The obtained accretion flow solution named the LHAF is described as an extension of the ADAF regime to high accretion rates and is found to be radiatively efficient (see also Yuan & Zdziarski 2004; Yuan et al. 2006). We can thus check if the luminosity range where we observe the steep correlation is compatible with the LHAF regime. We can write the X-ray luminosity of the accretion flow as $L_{\rm X} = \eta \dot{M} c^2$ with η the efficiency coefficient. η should be constant to get $L_{\rm X} \propto \dot{M}$, which is roughly the case for the LHAF (Yuan, private communication). Let us thus assume that H1743−322 is in the LHAF regime in the luminosity range where we observe the correlation of slope 1.4. According to Yuan (2001), an ADAF should become a LHAF when $\dot{M}$ exceeds the critical accretion rate $\dot{M}_{\rm crit} \sim 10\alpha_v^2 \dot{M}_{\rm Edd}$, where α_v is the viscosity coefficient and where we have defined the Eddington accretion rate as $\dot{M}_{\rm Edd} = L_{\rm Edd}/c^2$. For the standard value $\alpha_v = 0.1$, we thus have $\dot{M}_{\rm crit} \sim 0.1\dot{M}_{\rm Edd}$. Our results show that the steep correlation starts from a 3–100 keV luminosity $L_{\rm trans} \sim 5 \times 10^{-3} L_{\rm Edd}$. Then, for $L_{\rm X} = L_{\rm trans} = \eta \dot{M}_{\rm trans} c^2$, we have

$$\eta \dot{M}_{\rm trans} = 5 \times 10^{-3} \dot{M}_{\rm Edd}. \quad (4)$$

If $\dot{M}_{\rm trans}$ corresponds to the critical accretion rate $\dot{M}_{\rm crit}$ where the LHAF regime starts, then $\eta = 0.05$. The steep correlation is maintained up to the 3–100 keV luminosity $L_{\rm max} \sim 6 \times 10^{-2} L_{\rm Edd}$ where the intersection with the standard correlation occurs (see Fig. 5). If η is indeed constant in the LHAF regime, then for $L_{\rm X} = L_{\rm max}$, the corresponding accretion rate $\dot{M}_{\rm max}$ should be of the order of the Eddington accretion rate. The LHAF hypothesis thus leads to a high but not implausible value of the maximal accretion rate reached in the hard state.

Alternatively, we can estimate $\dot{M}_{\rm trans}$ from the radio luminosity and compare it to the critical accretion rate $\dot{M}_{\rm crit} \sim 0.1\dot{M}_{\rm Edd}$. Assuming $L_{\rm radio} \propto \dot{M}^{17/12}$ (equivalent to equation 2 in the case $\alpha = 0$ and $p = 2$), Körding, Fender & Migliari (2006b) found an estimate of the normalization constant between the radio luminosity of the compact jets and the accretion rate:

$$\dot{M} = \dot{M}_0 \left(\frac{L_{\rm radio}}{10^{30}\,{\rm erg\,s^{-1}}} \right)^{12/17} \text{with } \dot{M}_0 = 4.0 \times 10^{17}\,{\rm g\,s^{-1}}. \quad (5)$$

From Fig. 5, the radio luminosity corresponding to $L_{\rm trans}$ is $\sim 2.5 \times 10^{19}$ erg s^{-1} Hz^{-1}. Using equation (5) we thus derive $\dot{M}_{\rm trans} \sim 1.5 \times 10^{17}$ g s^{-1}. For a 10 $M_\odot$ black hole, this corresponds to $0.1\dot{M}_{\rm Edd}$, in agreement with the expected accretion rate at the transition to the LHAF regime. The LHAF model is thus a possible explanation for the behaviour of H1743−322 at high luminosity.

In a similar fashion, hot flow solutions have recently been found (Petrucci, private communication) for the jet emitting disc (JED) model (see e.g. Ferreira 2002, 2008; Ferreira et al. 2006; Combet & Ferreira 2008, and references therein), in which the flow goes from radiatively inefficient to radiatively efficient as the accretion rate increases. These JED hot solutions have properties very similar to those of one-temperature accretion flow studied by Esin et al. (1996) in the ADAF regime and revisited for higher accretion rates by Yuan et al. (2006) in the LHAF regime. The originality of the JED solutions resides in the fact that, by construction, they integrate self-consistently stationary and powerful self-collimated jets.

4.3.2 Accretion disc corona

Some ADC models could be also radiatively efficient in the hard state (see e.g. Galeev et al. 1979; Haardt & Maraschi 1991; Di Matteo et al. 1999; Malzac, Beloborodov & Poutanen 2001; Merloni

& Fabian 2002; Merloni 2003). In these models, a fraction f_c of the accretion power is dissipated in the corona, likely due to magnetic reconnection, and eventually emerges as X-ray radiation. The X-ray luminosity can be written as $L_X \sim f_c \dot{M} c^2$. In the case where the coronal plasma is heated by magnetic dissipation, Merloni & Fabian (2002) and Merloni (2003) have shown that f_c is constant when gas pressure dominates in the disc and therefore $L_X \propto \dot{M}$ which would explain the steep radio/X-ray correlation. When the radiation pressure dominates in the disc, Merloni et al. (2003) have shown that we should also expect a radio/X-ray correlation of the form $L_{radio} \propto L_X^{1.4}$. From the estimates of Merloni (2003), f_c should be of the order of 0.02 to 0.07 (for sub-Eddington systems) and would therefore be consistent with the X-ray luminosity range in which we observe the steep correlation.

From the radio/X-ray correlation point of view, ADC models could be therefore responsible for the X-ray emission in the high-luminosity hard state of H1743−322. However, the geometry assumed in these models leads naturally to the debate (beyond the scope of this paper) of whether or not the accretion disc extends close to the black hole.

4.3.3 Efficient to inefficient transition

When $L_X < L_{trans}$, our results suggest that H1743−322 undergoes a transition from the steep to the standard correlation. Under the assumptions on jet emission considered in this section, this transition to a relation $L_{radio} \propto L_X^{0.6}$ indicates that the accretion flow becomes radiatively inefficient, with $L_X \propto \dot{M}^{2-3}$ below L_{stand}. If we assume that equation (2) is valid during this transition (i.e. the radio luminosity is a good tracer of the accretion rate), the variation of radio luminosity between L_{trans} and L_{stand} should correspond to a variation of the accretion rate by a factor of ∼2. The corresponding variation of the X-ray luminosity is $L_{trans}/L_{stand} \sim 100$ and this transition occurs on a time-scale of 15 d. If the accretion rates varies little, as suggested by the almost constant level of radio emission during this transition, the radiative efficiency coefficient η of the accretion flow should vary significantly (by a factor of ∼50).

A transition from an efficient to an inefficient regime could be interpreted as a transition from an LHAF to an ADAF. In the framework of the ADC models, this could arise from changes in the properties of the corona heating mechanism. These details should be investigated on theoretical grounds.

Rather than being due to changes in the intrinsic properties of the accretion flow (as in the LHAF–ADAF case), the transition could results from the contribution of two emitting components, one inefficient with $L_X \propto \dot{M}^{2-3}$ and the other radiatively efficient with $L_X \propto \dot{M}$. When both components are present, the efficient component dominates the X-ray flux. Below a given $\dot{M}$ it disappears, leaving only the inefficient component. As an illustration, we can point to the work on XTE J1550−564 by Russell et al. (2010). The authors demonstrate the possibility that the origin of the X-ray emission evolves throughout the hard state, being alternatively dominated by thermal Comptonization or direct synchrotron emission from the compact jets. We also point out the work by Rodriguez et al. (2008a,b) on GRS 1915+105, where it is reported that two components are present in the hard X-ray spectrum during the plateau state. One of these components appears to be linked to the radio emission while the other is not. This supports the idea that several components co-exist and can dominate alternatively the X-ray band during the hard state. In our case, we could consider that above L_{trans} the X-ray emission is dominated by the contribution of an efficient accretion flow (as e.g. those mentioned previously). Below L_{stand}, the X-rays become dominated, for instance, by the synchrotron or SSC emission from the base of the jets.

4.3.4 The radio/X-ray diagram of BHXBs under the X-ray loud hypothesis

Regardless of the specific models that could explain our results, we can conclude that, as long as the assumptions about the jet physics stated in equations (2) and (3) are correct, the accretion flow has to be radiatively efficient (with $L_X \propto \dot{M}$) above $\sim 5 \times 10^{-3} L_{Edd}$. At lower X-ray luminosities, the radiative efficiency of the accretion flow should decrease significantly to reproduce the transition between the two correlations. Our results suggest that the X-ray luminosity scales as $\dot{M}^{2-3}$. If H1743−322 is indeed representative of the behaviour of the other outliers, we can thus represent the universal radio/X-ray diagram of BHXBs by the sketch shown in Fig. 7. This figure summarizes the X-ray loud interpretation. We can then distinguish two branches in the radio/X-ray diagram of BHXBs, according to the efficiency of the accretion flow and the consequent scaling of the X-ray luminosity with the mass accretion rate. For a still unknown reason, some BHXBs would remain radiatively inefficient in the hard state up to the transition to the soft state while others (the outliers) would develop a more radiatively efficient accretion flow leading them to follow the efficient branch. We also illustrate the possibility of the transition between branches below the critical accretion rate $\dot{M}_{trans}$.

If this sketch correctly describes the situation, the major issue to address now is to determine which fundamental parameter influences the global evolution of the accretion flow with mass accretion rate and will lead some black hole systems to follow the 'efficient' branch and others the 'inefficient' branch. In future works we thus need to investigate the influence of parameters such as the orbital period, the environment (e.g. magnetic) of the binary or perhaps the nature or evolutionary stage of the companion star. The physical conditions at outer boundary of the accretion disc could also have an influence on the dynamical and radiative structure of the flow (Yuan et al. 2000).

4.4 Beyond the standard assumptions on compact jet emission: the radio-quiet hypothesis

Another way to assess the problem would be to consider that the difference between the standard microquasars and the outliers arises from different jet properties rather than from different accretion flows. In this case we can relax the assumptions leading to equations (2) and (3).

We can first consider that the fraction f_j (in $Q_{jet} = f_j Q_{accr}$) of accretion energy injected into the jets is in fact dependent on the accretion rate. For simplicity, we will consider a linear dependence, $f_j \propto \dot{M}$. In that case, equation (3) becomes $L_{radio} \propto L_X^{2\xi/q}$. For a radiatively inefficient accretion flow ($q \sim 2$), this gives the correlation we observe for H1743−322.

Whether or not f_j is dependent on the accretion rate depends on the details of the jet launching mechanism e.g. mass loading into the jet, the specific acceleration mechanism or the origin of the magnetic field. A detailed theoretical study is therefore required to address this issue. However, as an example, if we consider the standard theories of magnetically driven jets, we note that the material is accelerated from a given region of the disc. The size of this region is usually

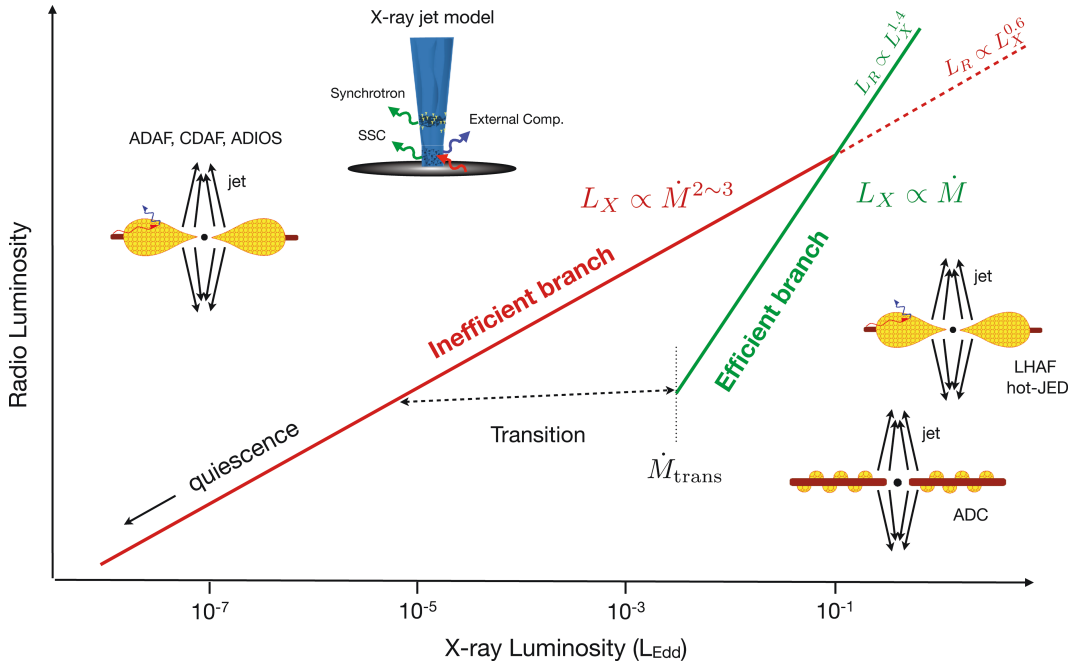

Figure 7. A schematic drawing of the global radio/X-ray correlation for Galactic black holes. The X-ray luminosity is expressed in terms of the Eddington luminosity for a 10 $M_\odot$ black hole. This figure illustrates the case where the correlation $L_{\rm radio} \propto L_{\rm X}^{1.4}$ of the outliers is a consequence of the coupling between a radiatively efficient accretion flow and a steady compact jet whose radio emission can be described by the relation $L_{\rm radio} \propto \dot{M}^{1.4}$. We distinguish two branches in this diagram according to the efficiency of the accretion flow and the consequent scaling of the X-ray luminosity with the mass accretion rate. The inefficient branch corresponds to the 'standard' radio/X-ray correlation observed for black holes systems like GX 339-4 or V404 Cyg. The inner flow in these systems can be described by e.g. a hot and inefficient accretion flow such as an ADAF, or by X-ray jet models as proposed by Markoff and collaborators. The efficient branch corresponds the radio/X-ray correlation of the outliers for which the X-ray luminosity in the hard state varies linearly with mass accretion rate. The X-ray emitting component in these systems could be described by e.g. a hot and efficient accretion flow such as the LHAF or hot-JED solutions or by some magnetic corona models. We also illustrate in this figure the possibility of a transition between the two branches as suggested by the behaviour of H1743−322. The pictures representing the different models are adapted from Markoff & Nowak (2004) and Nowak et al. (2004).

considered as constant in the models (and is often the entire disc). However, if we assume that, for any reason, this size evolves with accretion rate, it would therefore introduce a dependency of $f_{\rm j}$ on $\dot{M}$. This is however very speculative and we would have to explain why the size of this region changes in some systems and not in others.

Another parameter that could strongly influence the jet emission is of course the strength of the magnetic field embedded in the jet plasma. This will modify the synchrotron emission as a function of the jet power (equation 2). Pe'er & Casella (2009) presented a new model for jet emission in XRBs, in which they showed that the flux at radio wavelengths depends on the value of the magnetic field in a non-trivial way. Above a critical magnetic field strength, the outflowing electrons cool rapidly close to the jet base, leading to a strong suppression of the radio emission. Based on these results, Casella & Pe'er (2009) proposed that the outliers are sources with magnetic fields above the critical value. With respect to our results, it could also explain the transition phase between the two correlations. If we consider that the magnetic field strength evolves throughout the outburst (e.g. with the accretion rate), the transition could be due to the magnetic field decreasing below the critical value, leading H1743−322 to the same level of radio emission as GX 339-4 and V404 Cyg. However, the model does not explain precisely how the radio luminosity evolves with the injected power and thus with the accretion rate. Therefore, we cannot judge whether or not it is able to reproduce the correlation index of 1.4 we found. We thus encourage further developments of this model.

5 CONCLUSIONS

In this work we have studied the long-term radio/X-ray correlation of the BHC H1743−322. This source belongs to a group of Galactic black hole X-ray binaries dubbed as outliers of the 'universal' radio/X-ray correlation, for being located below the main $L_{\rm radio} \propto L_{\rm X}^{\sim0.5-0.7}$ relation. We therefore concentrated our efforts on providing new constraints and improving our understanding of these sources. Our main conclusions can be summarized as follows:

(i) In the brightest phase of the hard state, we find a tight power-law correlation with a slope $b = 1.38 \pm 0.03$, between the radio flux from the compact jets and the X-ray emission from the inner flow. This correlation is much steeper than usually found for black hole X-ray binaries and is the first precise measurement for an outlier.

(ii) When the source reaches a luminosity below $\sim 5 \times 10^{-3} L_{\rm Edd}\,(M/10\,{\rm M}_\odot)^{-1}$, we found evidence of a transition from the steep $b \sim 1.4$ relation to the standard $b \sim 0.6$ correlation seen in e.g. V404 Cyg and GX 339−4.

(iii) Additionally, we find that H1743−322 provides the best constraint to date (with a jet quenching factor of ∼700) supporting the idea of jet suppression during the soft state.

From these results, we discuss several hypotheses that could explain the correlation index along with the transition toward the standard correlation.

(i) We first show that if the standard scaling, $L_{\rm radio} \propto \dot{M}^{1.4}$, between the jet radio emission and the accretion rate is valid, then

our results require a radiatively efficient accretion flow that produces the X-ray emission in the hard state at high accretion rate. Ultimately, the flow has to become radiatively inefficient below a critical accretion rate, to account for the transition.

(ii) We also investigate the possibility that our results arise from the outflow properties of the source rather than from the accretion flow. We show in particular that if we relax the assumption that the jet power is a fixed fraction of the accretion power and we consider this fraction linearly dependent on the accretion rate, we can obtain the required correlation with an inefficient accretion flow.

Further investigations are now needed to determine which fundamental parameter of the binary systems or their environments can lead BHXBs of similar appearance to develop different accretion or ejection flows.

ACKNOWLEDGMENTS

MC and SC would like to thank Julien Malzac, Pierre-Olivier Petrucci, Elmar Körding, Sera Markoff, Feng Yuan and Michiel van der Klis for useful comments and discussions and Philip Edwards for prompt scheduling of the ATCA observations. The data on the 2009 outburst were collected by the JACPOT XRB collaboration (Miller-Jones et al. 2011), as part of an ongoing VLBA large project. In particular, the authors would like to acknowledge the roles played by Ron Remillard, Michael Rupen and Vivek Dhawan in this effort. The authors would also like to thank the anonymous referee for his critical reading that helped to improve the style and content of this paper.

The research leading to these results has received partial funding from the European Communitys Seventh Framework Programme (FP7/2007-2013) under grant agreement number ITN 215212 Black Hole Universe. This research has made use of data obtained from the High Energy Astrophysics Science Archive Research Center (HEASARC), provided by NASA's Goddard Space Flight Center. The ATCA is part of the Australia Telescope funded by the Commonwealth of Australia for operation as a National Facility managed by CSIRO. The National Radio Astronomy Observatory is a facility of the National Science Foundation operated under cooperative agreement by Associated Universities, Inc.

REFERENCES

Abramowicz M. A., Chen X., Granath M., Lasota J., 1996, ApJ, 471, 762
Achterberg A., Gallant Y. A., Kirk J. G., Guthmann A. W., 2001, MNRAS, 328, 393
Bell A. R., 1978, MNRAS, 182, 147
Belloni T. M., 2010, in Belloni T., ed., Lecture Notes in Physics, Vol. 794, States and Transitions in Black Hole Binaries. Springer-Verlag, Berlin, p. 53
Blandford R. D., Begelman M. C., 1999, MNRAS, 303, L1
Blandford R. D., Königl A., 1979, ApJ, 232, 34
Blandford R. D., Ostriker J. P., 1978, ApJ, 221, L29
Brocksopp C., Corbel S., Fender R. P., Rupen M., Sault R., Tingay S. J., Hannikainen D., O'Brien K., 2005, MNRAS, 356, 125
Cadolle Bel M. et al., 2007, ApJ, 659, 549
Capitanio F. et al., 2005, ApJ, 622, 503
Capitanio F., Belloni T., Del Santo M., Ubertini P., 2009, MNRAS, 398, 1194
Casella P., Pe'er A., 2009, ApJ, 703, L63
Chen Y. P., Zhang S., Torres D. F., Wang J. M., Li J., Li T. P., Qu J. L., 2010, A&A, 522, A99
Combet C., Ferreira J., 2008, A&A, 479, 481
Corbel S., Fender R. P., 2002, ApJ, 573, L35
Corbel S., Fender R. P., Tzioumis A. K., Nowak M., McIntyre V., Durouchoux P., Sood R., 2000, A&A, 359, 251
Corbel S. et al., 2001, ApJ, 554, 43
Corbel S., Nowak M. A., Fender R. P., Tzioumis A. K., Markoff S., 2003, A&A, 400, 1007
Corbel S., Fender R. P., Tomsick J. A., Tzioumis A. K., Tingay S., 2004, ApJ, 617, 1272
Corbel S., Kaaret P., Fender R. P., Tzioumis A. K., Tomsick J. A., Orosz J. A., 2005, ApJ, 632, 504
Corbel S., Tzioumis T., Coriat M., Brocksopp C., Fender R., 2008a, Astron. Telegram, 1766, 1
Corbel S., Körding E., Kaaret P., 2008b, MNRAS, 389, 1697
Coriat M., Corbel S., Buxton M. M., Bailyn C. D., Tomsick J. A., Körding E., Kalemci E., 2009, MNRAS, 400, 123
Coriat M. et al., 2011, in Romero G. E., Sunyaev R. A., Belloni T., eds, Proc. IAU Symp. 275, Jets at All Scales. Cambridge Univ. Press, Cambridge, p, 255
Di Matteo T., Celotti A., Fabian A. C., 1999, MNRAS, 304, 809
Drury L. O., Axford W. I., Summers D., 1982, MNRAS, 198, 833
Esin A. A., Narayan R., Ostriker E., Yi I., 1996, ApJ, 465, 312
Falcke H., Biermann P. L., 1995, A&A, 293, 665
Falcke H., Körding E., Markoff S., 2004, A&A, 414, 895
Fender R., 2006, Jets from X-Ray Binaries. Cambridge Univ. Press, Cambridge, p. 381
Fender R. P., Hendry M. A., 2000, MNRAS, 317, 1
Fender R. P., Kuulkers E., 2001, MNRAS, 324, 923
Fender R. et al., 1999, ApJ, 519, L165
Fender R. P., Belloni T. M., Gallo E., 2004, MNRAS, 355, 1105
Fender R. P., Homan J., Belloni T. M., 2009, MNRAS, 396, 1370
Ferreira J., 2002, in Bouvier J., Zahn J.-P., eds, EAS Publ. Ser. Vol. 3, Theory of Magnetized Accretion Discs Driving Jets. EDP Sciences, Les Ulis, p. 229
Ferreira J., 2008, New Astron. Rev., 52, 42
Ferreira J., Petrucci P., Henri G., Saugé L., Pelletier G., 2006, A&A, 447, 813
Galeev A. A., Rosner R., Vaiana G. S., 1979, ApJ, 229, 318
Gallant Y. A., Achterberg A., Kirk J. G., 1999, A&AS, 138, 549
Gallo E., Fender R. P., Pooley G. G., 2003, MNRAS, 344, 60
Galloway D. K., Psaltis D., Chakrabarty D., Muno M. P., 2003, ApJ, 590, 999
Haardt F., Maraschi L., 1991, ApJ, 380, L51
Hannikainen D. C., Hunstead R. W., Campbell-Wilson D., Sood R. K., 1998, A&A, 337, 460
Heinz S., Sunyaev R. A., 2003, MNRAS, 343, L59
Hjellming R. M., Johnston K. J., 1981, Nat, 290, 100
Hjellming R. M., Johnston K. J., 1988, ApJ, 328, 600
Homan J., Belloni T., 2005, Ap&SS, 300, 107
Homan J., Miller J. M., Wijnands R., van der Klis M., Belloni T., Steeghs D., Lewin W. H. G., 2005a, ApJ, 623, 383
Homan J., Buxton M., Markoff S., Bailyn C. D., Nespoli E., Belloni T., 2005b, ApJ, 624, 295
Ichimaru S., 1977, ApJ, 214, 840
Jahoda K., Markwardt C. B., Radeva Y., Rots A. H., Stark M. J., Swank J. H., Strohmayer T. E., Zhang W., 2006, ApJS, 163, 401
Jain R. K., Bailyn C. D., Orosz J. A., McClintock J. E., Remillard R. A., 2001, ApJ, 554, L181
Joinet A., Jourdain E., Malzac J., Roques J. P., Schönfelder V., Ubertini P., Capitanio F., 2005, ApJ, 629, 1008
Jonker P. G., Nelemans G., 2004, MNRAS, 354, 355
Jonker P. G. et al., 2010, MNRAS, 401, 1255
Kalemci E., Tomsick J. A., Rothschild R. E., Pottschmidt K., Corbel S., Kaaret P., 2006, ApJ, 639, 340
Kalemci E., Tomsick J. A., Yamaoka K., Ueda Y., 2008, Astron. Telegram, 1348
Kaluzienski L. J., Holt S. S., 1977, IAU Circular, 3099, 3
Körding E., Falcke H., Corbel S., 2006a, A&A, 456, 439
Körding E. G., Fender R. P., Migliari S., 2006b, MNRAS, 369, 1451
Krimm H. A. et al., 2009, Astron. Telegram, 2058, 1

Lutovinov A., Revnivtsev M., Molkov S., Sunyaev R., 2005, A&A, 430, 997
McClintock J. E., Remillard R. A., 2006, Black Hole Binaries. Cambridge Univ. Press, Cambridge, p. 157
McClintock J. E., Remillard R. A., Rupen M. P., Torres M. A. P., Steeghs D., Levine A. M., Orosz J. A., 2009, ApJ, 698, 1398
Malzac J., Beloborodov A. M., Poutanen J., 2001, MNRAS, 326, 417
Malzac J., Belmont R., Fabian A. C., 2009, MNRAS, 400, 1512
Markoff S., Nowak M. A., 2004, ApJ, 609, 972
Markoff S., Falcke H., Fender R., 2001, A&A, 372, L25
Markoff S., Nowak M., Corbel S., Fender R., Falcke H., 2003, A&A, 397, 645
Markoff S., Nowak M. A., Wilms J., 2005, ApJ, 635, 1203
Markwardt C. B., Swank J. H., 2003, Astron. Telegram, 133
Merloni A., 2003, MNRAS, 341, 1051
Merloni A., Fabian A. C., 2002, MNRAS, 332, 165
Merloni A., Heinz S., di Matteo T., 2003, MNRAS, 345, 1057
Migliari S., Fender R. P., 2006, MNRAS, 366, 79
Miller J. M. et al., 2006, ApJ, 646, 394
Miller-Jones J. C. A., Jonker P. G., Dhawan V., Brisken W., Rupen M. P., Nelemans G., Gallo E., 2009, ApJ, 706, L230
Miller-Jones J. C. A. et al., 2010, ApJ, 716, L109
Miller-Jones J. C. A. et al., 2011, in Romero G. E., Sunyaev R. A., Belloni T., eds, Proc. IAU Symp. 275, Jets at All Scales. Cambridge Univ. Press, Cambridge, p. 224
Mirabel I. F., Rodriguez L. F., 1994, Nat, 371, 46
Motta S., Muñoz-Darias T., Belloni T., 2011, MNRAS, doi:10.1111/j.1365-2966.2011.18483.x
Muno M. P., Belloni T., Dhawan V., Morgan E. H., Remillard R. A., Rupen M. P., 2005, ApJ, 626, 1020
Narayan R., Yi I., 1994, ApJ, 428, L13
Nowak M. A., Wilms J., Pottschmidt K., Pooley G. G., 2004, BAAS, 36, 946
Parmar A. N., Kuulkers E., Oosterbroek T., Barr P., Much R., Orr A., Williams O. R., Winkler C., 2003, A&A, 411, L421
Pe'er A., Casella P., 2009, ApJ, 699, 1919
Prat L. et al., 2009, A&A, 494, L21
Rodriguez J., Cadolle Bel M., Tomsick J. A., Corbel S., Brocksopp C., Paizis A., Shaw S. E., Bodaghee A., 2007, ApJ, 655, L97
Rodriguez J. et al., 2008a, ApJ, 675, 1436
Rodriguez J. et al., 2008b, ApJ, 675, 1449
Rupen M. P., Mioduszewski A. J., Dhawan V., 2004, Astron. Telegram, 314, 1
Rupen M. P., Mioduszewski A. J., Dhawan V., 2005, Astron. Telegram, 575, 1
Rupen M. P., Dhawan V., Mioduszewski A. J., 2008a, Astron. Telegram, 1352, 1
Rupen M. P., Dhawan V., Mioduszewski A. J., 2008b, Astron. Telegram, 1384, 1
Rushton A., Spencer R., Fender R., Pooley G., 2010, A&A, 524, A29
Russell D. M., Fender R. P., Hynes R. I., Brocksopp C., Homan J., Jonker P. G., Buxton M. M., 2006, MNRAS, 371, 1334
Russell D. M., Maccarone T. J., Körding E. G., Homan J., 2007, MNRAS, 379, 1401
Russell D. M., Maitra D., Dunn R. J. H., Markoff S., 2010, MNRAS, 405, 1759
Rybicki G. B., Lightman A. P., 1979, Radiative Processes in Astrophysics. Wiley Interscience, New York, p. 395
Sault R. J., Wieringa M. H., 1994, A&AS, 108, 585
Sault R. J., Teuben P. J., Wright M. C. H., 1995, in Shaw R. A., Payne H. E., Hayes J. J. E., eds, ASP Conf. Ser. Vol. 77, Astronomical Data Analysis Software and Systems IV. Astron. Soc. Pac., San Francisco, p. 433
Shakura N. I., Sunyaev R. A., 1973, A&A, 24, 337
Soleri P. et al., 2010, MNRAS, 406, 1471
Swank J., 2004, Astron. Telegram, 301, 1
Tanaka Y., Shibazaki N., 1996, ARA&A, 34, 607
Tudose V., Fender R. P., Linares M., Maitra D., van der Klis M., 2009, MNRAS, 400, 2111
van der Klis M., 2006, Rapid X-Ray Variability. Cambridge Univ. Press, Cambridge, p. 39
Xue Y. Q., Cui W., 2007, A&A, 466, 1053
Yamaoka K. et al., 2009, Astron. Telegram, 2364, 1
Yuan F., 2001, MNRAS, 324, 119
Yuan F., Zdziarski A. A., 2004, MNRAS, 354, 953
Yuan F., Peng Q., Lu J., Wang J., 2000, ApJ, 537, 236
Yuan F., Taam R. E., Xue Y., Cui W., 2006, ApJ, 636, 46
Zdziarski A. A., Gierliński M., Mikołajewska J., Wardziński G., Smith D. M., Harmon B. A., Kitamoto S., 2004, MNRAS, 351, 791

This paper has been typeset from a TEX/LATEX file prepared by the author.